Journal of ELECTRONIC MATERIALS, Vol. 39, No. 5, 2010
DOI: 10.1007/s11664-009-1022-x
© 2009 The Author(s). This article is published with open access at Springerlink.com

# Properties of In-Doped ZnO Films Grown by Metalorganic Chemical Vapor Deposition on GaN(0001) Templates

TAMMY BEN-YAACOV,[1,3] TOMMY IVE,[1] CHRIS G. VAN DE WALLE,[1] UMESH K. MISHRA,[2] JAMES S. SPECK,[1] and STEVEN P. DENBAARS[1,2]

1.—Materials Department, University of California, Santa Barbara, CA 93106, USA. 2.—Electrical and Computer Engineering Department, University of California, Santa Barbara, CA 93106, USA. 3.—e-mail: tammy@umail.ucsb.edu

We investigated the properties of indium-doped zinc oxide layers grown by metalorganic chemical vapor deposition on semi-insulating GaN(0001) templates. Specular and transparent films were grown with *n*-type carrier concentrations up to $1.82 \times 10^{19}$ cm$^{-3}$ as determined by Hall measurements, and all In-doped films had carrier concentrations significantly higher than that of a comparable undoped film. For low In flows, the carrier concentration increased accordingly with trimethyl-indium (TMIn) flow until a maximum carrier concentration of $1.82 \times 10^{19}$ cm$^{-3}$ was realized. For higher In flows, the carrier concentration decreased with increasing TMIn flow rate. Sheet resistance as low as 185 Ω/sq was achieved for the In-doped films, which is a significant decrease from that of a comparable undoped ZnO film. Our *n*-type doping studies show that In is an effective dopant for controlling the *n*-type conductivity of ZnO.

**Key words:** ZnO, zinc oxide, doping, *n*-type, MOCVD, metalorganic chemical vapor deposition, ZnO:In, indium doping, electrical characterization, growth, crystal growth, thin films

ZnO has many unique electrical, piezoelectric, and optical properties[1–3] which make it an applicable material for optoelectronic devices. For this reason, there is a widespread effort toward epitaxial growth of high-quality, single-crystal ZnO thin films, as well as much work on controlling the electrical properties of these films. ZnO has a wide direct bandgap of 3.4 eV, and it crystallizes in the wurtzite structure. It has an exciton binding energy of 60 meV,[4] and so it has the potential for stable and efficient optical emission at room temperature. The availability of high-quality bulk ZnO substrates opens the possibility for homoepitaxial growth. These properties make ZnO an excellent candidate for various device applications.

For ZnO to be used for optoelectronic applications, it is necessary to control the *n*-type conductivity of ZnO films, while simultaneously achieving good surface morphology and crystal quality. This is a major challenge, as undoped ZnO almost always exhibits *n*-type conductivity, and there is a significant body of work toward identifying the cause of high unintentional conductivity (see Refs. 5–7 and references therein). In addition, the introduction of dopants has a strong impact on film morphology and crystal quality.

For II–VI compound semiconductors including ZnO, group III elements, including In, Ga, and Al, are regarded as ideal donors due to their valence.[8,9] Most efforts reported on *n*-type doping of ZnO are for transparent contact applications, with Ga as the dopant. It has been reported that thin ZnO:Ga layers work well as a contact to *p*-GaN in InGaN light-emitting diodes (LEDs), and that they improve the light extraction efficiency of the devices.[10] We have grown such structures and also realized promising results with thin ZnO:Ga layers as contacts to InGaN LEDs.[11] Little work has been reported, however, on controlled *n*-type doping of thicker single-crystal ZnO films.

(Received August 1, 2009; accepted November 19, 2009; published online December 11, 2009)

There is a lot of effort toward fabricating high-quality ZnO contacts with high conductivity, low resistivity, and high transparency in nitride-based devices such as LEDs and solar cells. Thin-film metals have been widely studied as contact materials to $p$-type GaN, Ni/Au being the most common. The efficiency of these devices is partly limited by absorption in the semi-transparent $p$-contact Ni/Au layer, and therefore it is of interest to implement transparent conducting oxides (TCO) as an alternative contact scheme.[12] The dominant TCO is amorphous indium tin oxide (ITO), most commonly deposited by sputtering techniques.[13–16] Due to the deposition technique and material quality, it has been shown that there is usually a high contact resistance at the $p$-GaN/ITO interface, and consequently ITO-contacted LEDs exhibited a significantly higher turn-on voltage than that of metal-contacted devices.[13] ZnO has the potential to be a more favorable candidate than ITO in this regard, because the $a$-axis lattice constant of ZnO is closely matched to that of GaN, and so high-quality ZnO films can be grown epitaxially on GaN.[17,18] There is also great economical motivation for implementing ZnO as a contact over ITO, as the price of In has been rising and is significantly higher than the price of Zn.

The ability to control the $n$-type conductivity of high-quality ZnO films while sustaining good crystal quality and surface morphology is invaluable for device applications. In this study, we present the properties of 0.5-$\mu$m-thick In-doped ZnO(0001) films grown by metalorganic chemical vapor deposition (MOCVD) on Fe-doped, semi-insulating GaN(0001) templates.

A Thomas Swan close-coupled showerhead MOCVD reactor was used for the growth experiments. Diethyl-zinc (DEZ), trimethyl-indium (TMIn), and pure $O_2$ were the Zn, In, and oxygen sources, respectively. Nitrogen was used as the carrier gas. Fe-doped, semi-insulating $GaN/Al_2O_3$ templates from LUMILOG were used as substrates for these growth experiments, which allowed for electrical isolation of the ZnO film.

An undoped ZnO buffer layer was deposited at 450°C with a reactor pressure of 50 torr before the temperature was increased to 950°C for the high-temperature deposition of the ZnO epitaxial layer. At 950°C, a thin unintentionally doped (UID) ZnO layer was deposited first, and then In was introduced for the growth of a thicker ZnO:In layer. Figure 1a shows a diagram of the growth structure. The total thickness of the ZnO layers was 0.5 $\mu$m. The VI/II ratio was 550 and 11,000 for the buffer layer and the high-temperature epitaxial layer, respectively. The TMIn flows ranged from 3 sccm to 50 sccm. The growth rate was 2.2 Å/s. These growth conditions were realized by an extensive heteroepitaxial growth study of undoped ZnO films grown on GaN(0001) templates, which was conducted prior to the In-doping experiments. These growth conditions yielded UID ZnO layers with locally straight steps indicating step-flow growth, and a root-mean-square roughness less than 2.6 nm (20 $\mu$m × 20 $\mu$m). The full-width at half-maximum (FWHM) across the symmetric (0002) x-ray rocking curve was as narrow as 0.091°.[19] We compared the electrical properties, the film and surface morphology, and the crystal quality of the In-doped films with a comparable undoped film to clearly see the effects of the In doping.

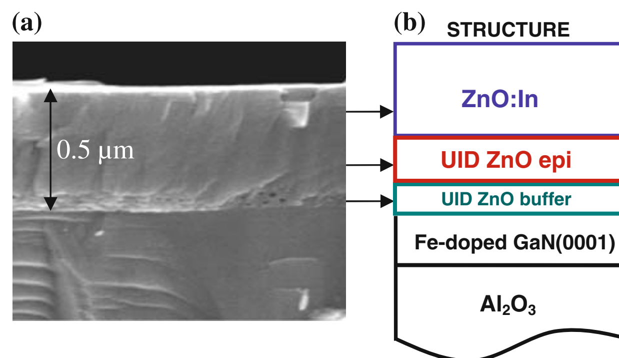


Fig. 1. (a) Cross-sectional SEM image of sample C (Table I) with the layer structure outlined to the right. (b) Growth structure for ZnO In-doping experiments. The growth sequence on Fe-doped, semi-insulating GaN(0001) templates is as follows: (1) undoped ZnO buffer, (2) undoped ZnO epilayer, (3) In-doped ZnO epilayer. The epilayer growth temperature and reactor pressure were 950°C and 50 torr, respectively.

Figure 1a shows a cross-sectional scanning electron microscopy (SEM) image of a ZnO:In film doped with 5 sccm TMIn, with the layer structure shown in Fig. 1b. In this image it is possible to clearly see the ZnO/GaN interface, the buffer layer, and the epilayer. No interface was observed between the UID ZnO and the In-doped ZnO, and In incorporation had negligible impact on the film morphology.

Table I shows the properties of both a UID ZnO film (sample A) and of the In-doped films grown in this study (samples B–K). Carrier concentration, mobility, and sheet resistance were evaluated by Hall measurements using the Van der Pauw configuration with In dots. All In-doped films had carrier concentrations significantly greater than that of the undoped sample, as the range of carrier concentration for In-doped samples was $5.3 \times 10^{18}$ cm$^{-3}$ to $1.8 \times 10^{19}$ cm$^{-3}$, as compared with $5.4 \times 10^{17}$ cm$^{-3}$ for the undoped sample.

The sheet resistances of the In-doped ZnO films were significantly lower than that of the undoped sample. A minimum sheet resistance of 184 Ω/sq was achieved for sample C, as compared with 3100 Ω/sq for the undoped sample. For comparison, the sheet resistances for 200-nm-thick sputtered and e-beam-deposited ITO films have been reported to be as low as 15 Ω/sq and 33 Ω/sq, respectively.[15] The ZnO:In film, which is more than double the thickness of these ITO films, has a sheet resistance greater by only a factor of about 6. With some further improvement, In-doped ZnO will be able to compete with ITO in terms of resistivity.

**Table I. Summary of properties of the In-doped ZnO layers presented in this study**

| Sample | TMIn Flow (sccm) | $n_{Hall}$ ($cm^{-3}$) | [In] ($cm^{-3}$) | $\mu$ ($cm^2$/Vs) | $R_{sheet}$ (Ω/sq) | $\Delta\omega$ (0002) (degree) |
|---|---|---|---|---|---|---|
| A (undoped) | 0 | $5.4 \times 10^{17}$ | $1.4 \times 10^{18}$ | 37 | 3100 | 0.091 |
| B | 3 | $5.32 \times 10^{18}$ | $1.0 \times 10^{19}$ | 38 | 622 | 0.136 |
| C | 3.6 | $1.0 \times 10^{19}$ | – | 37 | 540 | – |
| D | 4.1 | $1.36 \times 10^{19}$ | – | 37 | 348 | 0.146 |
| E | 4.6 | $1.6 \times 10^{19}$ | – | 38 | 206 | – |
| F | 5 | $1.82 \times 10^{19}$ | $3.7 \times 10^{19}$ | 37 | 184 | 0.153 |
| G | 6 | $1.79 \times 10^{19}$ | $8.0 \times 10^{19}$ | 35 | 198 | 0.165 |
| H | 12 | $1.39 \times 10^{19}$ | $1.3 \times 10^{20}$ | 35 | 262 | 0.177 |
| I | 25 | $1.38 \times 10^{19}$ | $4.0 \times 10^{20}$ | 30 | 299 | 0.181 |
| J | 35 | $1.12 \times 10^{19}$ | $5.5 \times 10^{20}$ | 45 | 245 | 0.182 |
| K | 50 | $7.7 \times 10^{18}$ | $6.0 \times 10^{20}$ | 33 | 489 | – |

Listed are donor concentration ($n_{Hall}$), mobility ($\mu$), and sheet resistance ($R_{sheet}$) as determined by Hall measurements, the indium concentration ([In]) as determined by secondary-ion mass spectroscopy (SIMS), and the x-ray diffraction (XRD) FWHM $\Delta\omega$ of the ZnO(0002) reflection.

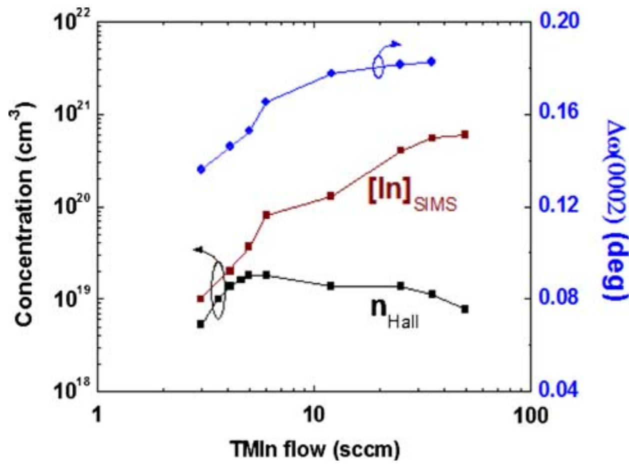


Fig. 2. Dependence of electron concentration (measured by Hall effect) and In concentration (measured with SIMS) on TMIn flow (left $y$-axis), and the FWHM $\Delta\omega$ of rocking curves for the (0002) reflection as a function of TMIn flow (right $y$-axis).

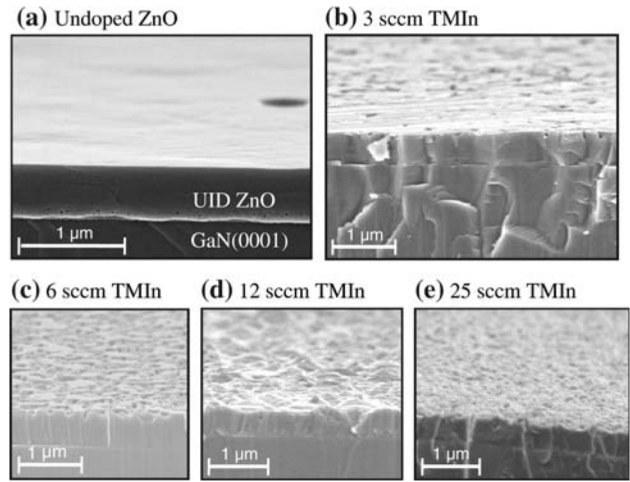


Fig. 3. SEM images of (a) a UID ZnO layer and (b–e) ZnO:In films grown on GaN(0001) templates, showing the effect of In doping on surface morphology. All ZnO:In films are homogeneous and compact, and surface morphology improves for lower In flows: (a) sample A; film is smooth, hexagonal pit can be observed; (b) sample B, (c) sample G, (d) sample H, and (e) sample I.

The dependence of electron concentration, as measured by Hall effect, and chemical In concentration, measured with secondary-ion mass spectroscopy (SIMS), on TMIn flow is shown in Fig. 2. For low In flows, the electron concentration increased as the dopant flow increased, in good agreement with the In concentration measured by SIMS. The highest electron concentration ($1.8 \times 10^{19}$ $cm^{-3}$) was realized for sample C. When the In concentration was increased beyond this concentration the measured electron concentration decreased, which may indicate that much of the In was not incorporated as a simple shallow donor.

The In concentration as measured by SIMS scaled roughly with TMIn flow and varied between $1 \times 10^{19}$ $cm^{-3}$ and $6 \times 10^{20}$ $cm^{-3}$. The samples with higher In concentrations were overdoped, i.e., the In concentration was so high that the material quality began to degrade. The crystal quality was assessed by recording the FWHM of XRD $\omega$-scans across the symmetric (0002) reflection. Table I summarizes the results from these measurements, and Fig. 2 also shows the dependence of FWHM $\Delta\omega$ of the rocking curves on the TMIn flow. The ZnO:In films have good crystal quality, as sample B had a narrow FWHM of 0.136° (489 arcseconds), and it is clear that the quality of the ZnO:In films decreased with increasing TMIn flow.

SEM images were used to evaluate the effect of In on film and surface morphology. Figure 3 shows the undoped film (a), and four In-doped films (b–e) for a range of TMIn flows. The undoped ZnO film was very smooth with occasional hexagonal pits, as shown in Fig. 3a. As shown in Fig. 3b, the introduction of 3 sccm of TMIn, which was in the low part of the doping range for this experimental series, had a noticeable impact on the surface morphology, which became slightly rougher. Figure

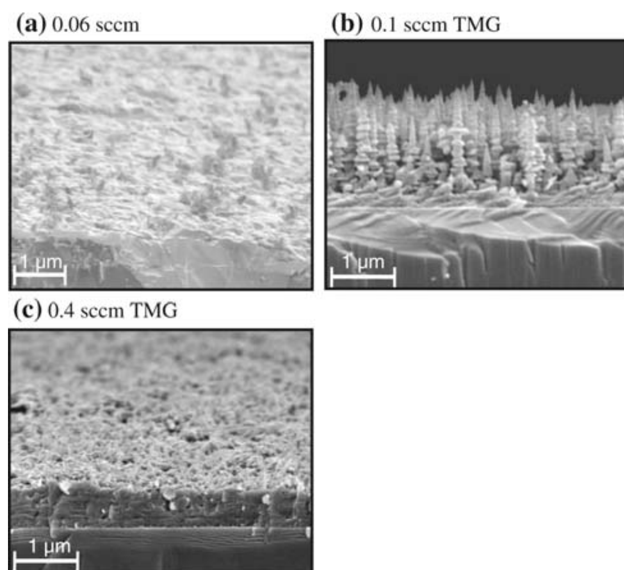


Fig. 4. SEM images of ZnO:Ga films grown on GaN(0001) templates, showing the effect of Ga doping on film and surface morphology. Ga has a profound and negative impact on morphology. (a) ZnO:Ga, TMG flow = 0.06 sccm; surface extremely rough, granular morphology. (b) ZnO:Ga, TMG flow = 0.1 sccm; columnar screw-like morphology. (c) ZnO:Ga, TMG flow = 0.4 sccm; layer is full of holes, granular.

3c–e shows samples with TMIn flows of 6 sccm, 12 sccm, and 25 sccm, respectively. In the overdoped regime, the morphology degraded, as hexagonal pits and hillocks were observed. One very important feature of all the In-doped films was that the film remained homogeneous and never displayed a columnar structure. A companion doping study using Ga as the *n*-type dopant consistently yielded ZnO films with columnar microstructure.

Experiments with Ga doping were performed prior to the In-doping study, using the same growth conditions, but with the injection of trimethylgallium (TMG) in the range of 0.06 sccm to 0.4 sccm, which is in the heavy doping range. For this range of TMG flows, the carrier concentration of the films did not increase. The sample grown with 0.06 sccm TMG ([Ga] $\sim 10^{21}$ cm$^{-3}$ as measured by SIMS) was the only one to which we were able to contact successfully. It had a carrier concentration of $8.8 \times 10^{16}$ cm$^{-3}$, which corresponds to the unintentional background doping. The sheet resistance and mobility of this sample were $1.2 \times 10^{4}$ Ω/sq and 20 cm$^2$/Vs, respectively.

Figure 4 shows SEM images of the Ga-doped ZnO layers grown in this study. It is clear that Ga, even at such low injection levels, had a profound and deleterious impact on film morphology, as these layers were granular, extremely rough, and the sample shown in Fig. 4b had a columnar screw-like morphology.

We performed an experimental study on In doping of ZnO(0001) films on GaN(0001) templates. The peak carrier concentration realized was $1.82 \times 10^{19}$ cm$^{-3}$, and a minimum sheet resistance of 184 Ω/sq was achieved. Indium is an effective dopant for controlling the *n*-type conductivity of ZnO grown on GaN(0001) templates, and it is now of interest to implement these films as contacts to nitride-based devices. We are conducting studies to understand the cause of the microstructural degradation of the ZnO:In films, investigating the optical properties of these films, and developing high-quality In-doped ZnO contacts to *n*-type and *p*-type GaN. Also, we are exploring additional film deposition conditions and growth structures to further drive up the conductivity of the ZnO:In films so that they can compete with ITO films. For example, we are investigating how varying growth temperature and VI/II ratio can promote indium incorporation. We are also growing ZnO:In films with In-doped buffer layers rather than UID buffers and are also directly depositing epitaxial films without the use of a buffer layer, with the goal of further increasing the conductivity of the In-doped ZnO films.

## ACKNOWLEDGEMENTS

This work was supported by MRSEC Program of the National Science Foundation under Award No. DMR05-20415 and by SSLEC.

## OPEN ACCESS

This article is distributed under the terms of the Creative Commons Attribution Noncommercial License which permits any noncommercial use, distribution, and reproduction in any medium, provided the original author(s) and source are credited.

## REFERENCES

1. W.H. Hirschwald, *Acc. Chem. Res.* 18, 228 (1985).
2. U. Özgür, Y.I. Alivov, and C. Liu, *J. Appl. Phys.* 98, 4130 (2005).
3. S.J. Pearton, C.R. Abernathy, and M.E. Overberg, *J. Appl. Phys.* 93, 1 (2003).
4. D.G. Thomas, *J. Phys. Chem. Solids* 15, 86 (1960).
5. A. Janotti and C.G. Van de Walle, *Appl. Phys. Lett.* 87, 122102 (2005).
6. D.C. Look, J.W. Hemsky, and F.R. Sizelove, *Phys. Rev. Lett.* 82, 2552 (1999).
7. C.G. Van de Walle, *Phys. Rev. Lett.* 85, 1013 (2000).
8. V. Bhosle, A. Tiwari, and J. Narayan, *Appl. Phys. Lett.* 88, 032106 (2006).
9. W. Sato, Y. Itsuki, and S. Morimoto, *Phys. Rev. B* 78, 045219 (2008).
10. K. Tamura, K. Nakahara, and M. Sakai, *Phys. Status Solidi* 201, 2704 (2004).
11. T. Ive, T. Ben-Yaacov, A. Murai, H. Asamizu, and J.S. Speck, *Phys. Status Solidi* 5, 3091 (2008).
12. K. Nakahara, *Jpn. J. Appl. Phys.* 43, L180 (2004).
13. T. Margalith, O. Buchinsky, and L.A. Coldren, *Appl. Phys. Lett.* 74, 3930 (1999).
14. C. Guillen and J. Herrero, *J. Appl. Phys.* 101, 073514 (2007).
15. L. Kerkache, A. Layadi, E. Dogheche, and D. Remiens, *Eur. Phys. J. Appl. Phys.* 39, 1 (2007).
16. UCSB unpublished results.
17. M.A.L. Johnson, S. Fujita, and W.H. Rowland, *J. Electron. Mater.* 25, 855 (1996).
18. H.J. Ko, Y.F. Chen, S.K. Hong, H. Wenisch, T. Yao, and D.C. Look, *Appl. Phys. Lett.* 77, 3761 (2000).
19. T. Ive, T. Ben-Yaacov, and J. Speck, *J. Cryst. Growth* 310, 3407 (2008).